

Supporting Information (SI)

**A 'turn-on' coordination based detection of Pd<sup>2+</sup> - Application in Bioimaging**

**Paramjit Kaur,<sup>a\*</sup> Navdeep Kaur,<sup>a</sup> Mandeep Kaur,<sup>a</sup> Vikram Dhuna,<sup>b</sup> Jatinder Singh<sup>b</sup> and Kamaljit Singh,<sup>a\*</sup>**

<sup>a</sup>Department of Chemistry, UGC-Centre of Advanced Studies-I, <sup>b</sup>Department of Molecular Biology and Biochemistry, Guru Nanak Dev University, Amritsar-143 005, Punjab, India.

E-mail: [paramjit19in@yahoo.co.in](mailto:paramjit19in@yahoo.co.in); [kamaljit19in@yahoo.co.in](mailto:kamaljit19in@yahoo.co.in)

**Table of Contents**

<b>1.</b> General note to physical measurements.	<b>S1</b>
<b>2.</b> Quantum yield calculations.	<b>S1</b>
<b>3.</b> Detection limit calculations.	<b>S2</b>
<b>4.</b> Computational details.	<b>S2</b>
<b>5.</b> Cell imaging material and method.	<b>S2</b>
<b>6.</b> Synthesis and characterization of compounds.	<b>S3-S5</b>
<b>7.</b> <sup>1</sup> H NMR spectrum of <b>1</b> .	<b>S6</b>
<b>8.</b> Mass spectrum of <b>1</b> .	<b>S6</b>
<b>9.</b> IR (KBr) spectrum of <b>1</b> .	<b>S7</b>
<b>10.</b> <sup>13</sup> C NMR spectrum of <b>1</b> .	<b>S7</b>
<b>11.</b> Expanded <sup>13</sup> C NMR spectrum (in parts) copied from original software(Alice).	<b>S8</b>
<b>12.</b> Changes in the emission properties of <b>1</b> upon pH titration with HCl and NaOH.	<b>S9</b>
<b>13. Theoretical Calculations</b>	
(a) Selected data of electronic transitions in <b>1</b> by TD-DFT calculations and contour surfaces of the corresponding orbitals.	<b>S9</b>
(b) Selected data of electronic transitions in <b>1</b> :Pd <sup>2+</sup> by TD-DFT calculations and contour surfaces of the corresponding orbitals	<b>S10</b>
(c) Cartesian coordinates of the optimized structure of <b>1</b> .	<b>S11-S13</b>
(d) Cartesian coordinates of the optimized structure of <b>1</b> :Pd <sup>2+</sup> .	<b>S13-16</b>
<b>14.</b> Mass spectrum of <b>1</b> :Pd <sup>2+</sup> .	<b>S16</b>
<b>15.</b> <sup>1</sup> H NMR spectrum of <b>1</b> :Pd <sup>2+</sup> .	<b>S17</b>
<b>16.</b> Changes in the chemical shift of NMR peaks of <b>1</b> upon addition of Pd <sup>2+</sup> .	<b>S17</b>
<b>17.</b> Representative detection limits for palladium reported in literature.	<b>S18</b>
<b>18.</b> Changes in the emission properties of <b>1</b> upon addition of Pd <sup>2+</sup> in the presence	<b>S18</b>

of various metal ions.

<b>19.</b> Changes in the emission spectrum of <b>1</b> upon addition of $\text{Hg}^{2+}$ .	<b>S19</b>
<b>20.</b> Changes in the absorption spectra of <b>1</b> upon addition of $\text{Hg}^{2+}$ .	<b>S19</b>
<b>21.</b> Changes in the absorption spectra of <b>1</b> , upon sequential addition of $\text{Pd}^{2+}$ in the presence of $\text{Hg}^{2+}$ and cysteine.	<b>S20</b>
<b>22.</b> LOGIC GATE	<b>S20</b>
<b>23.</b> Reversibility experiments of <b>1</b> upon addition $\text{Na}_2\text{S}$ in solution of <b>1</b> : $\text{Pd}^{2+}$ .	<b>S21</b>
<b>24.</b> Confocal images of MCF-7 cells, supplemented with various concentration of $\text{Pd}^{2+}$ .	<b>S21</b>
<b>25.</b> References.	<b>S22-S23</b>

**General note to physical measurements:**

IR spectra were recorded on a Perkin Elmer Spectrum Two-IR Fourier-Transform spectrophotometer in the range 400-4000  $\text{cm}^{-1}$  using KBr as medium.  $^1\text{H}$  NMR (300 MHz) and  $^{13}\text{C}$  NMR (75 MHz) spectra were recorded in  $\text{CDCl}_3$  and  $\text{CD}_3\text{CN}$  on a JEOL-FT NMR-AL. Tetramethylsilane (TMS) served as the internal standard (0 ppm for  $^1\text{H}$  and 77.0 ppm for  $^{13}\text{C}$ ). Data are reported as follows: chemical shift in ppm ( $\delta$ ), integration, multiplicity (s=singlet, d=doublet), coupling constant  $J$  (Hz) and assignment. Mass spectra were recorded on a microTOF-Q II 10356 spectrometer. The purity of the products was checked by elemental analysis performed on a ThermoFisher EA1112 CHNS analyzer and were within  $\pm 0.4\%$  of the theoretical values. Melting points were determined in open capillaries and are uncorrected. Emission studies were made on Perkin Elmer LS 55 Fluorescence Spectrometer with excitation slit width as 10.0 and emission slit width as 2.5 with off emission correction mode. UV-Vis spectra were recorded on a SHIMADZU 1601 PC spectrophotometer, with a quartz cuvette (path length, 1 cm) and studies were performed in AR grade THF. The cell holder of the spectrophotometer was maintained at  $25^\circ\text{C}$  for consistency in the recordings. The cell imaging was carried out on the NIKON A1R confocal microscope.

**Quantum yield calculations:**

The fluorescence quantum yields were measured with respect to 9, 10-diphenylanthracene as standard having quantum yield of 0.86 in cyclohexane.<sup>1</sup>

$$\Phi_u = \Phi_s \cdot F_u \cdot A_s \cdot \eta_u^2 / F_s \cdot A_u \cdot \eta_s^2$$

$\Phi$  = quantum yield

F = Integrated fluorescence intensity

A = Absorbance

H = refractive index of solvent

s = standard i.e. 9, 10-diphenylanthracene

u = sample

**Detection limit calculations:**

The detection limit was calculated on the basis of the fluorescence titration. The fluorescence emission spectrum of **1** was measured 6 times, and the standard deviation of blank measurement was achieved. To gain the slope, the ratio of emission intensity at 520 nm was plotted as a concentration of Pd<sup>2+</sup>. The detection limit was calculated using the following equation.

$$\text{Detection limit} = 3 \times \sigma / K$$

Where  $\sigma$  is the standard deviation of blank measurement, and K is the slope between the ratio of emission intensity versus [Pd<sup>2+</sup>].

**Computational details:**

All theoretical calculations were carried out by using the Gaussian 09 suite of programs.<sup>2</sup> The molecular geometries of the chromophores were optimized at the DFT method employing the hybrid B3LYP<sup>3</sup> functional. 6-31G\* basis set was used for C, H, B, F, Cl, N, S, and O atoms whereas SDD with effective core potential for the metal atom Pd<sup>2+</sup>. The same model chemistry was used for the calculation of the properties of the chromophores. The first 50 excited states were calculated by using time-dependent density functional theory (TD-DFT calculations). The molecular orbital contours were plotted using Gauss view 5.0.9.

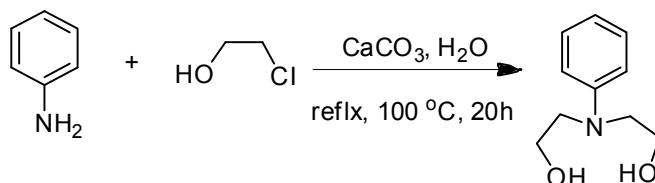
**Cell imaging materials and methods**

Human breast adenocarcinoma MCF7 cell line was obtained from NCCS, Pune, India and maintained on Dulbecco's Modified Eagle's Medium (DMEM) supplemented with streptomycin (100 U/ml), gentamycin (100 µg/ml), 10% FBS (Sigma-Aldrich) at 37 °C and humid environment containing 5% CO<sub>2</sub>.

For imaging, MCF7 cells were cultured on 18 mm glass coverslips in 12 well plates at  $2 \times 10^4$  cells/well and allowed to grow for 48 hours (till 70-80% confluence). Experiments to assess Pd<sup>2+</sup> uptake were performed in the same media supplemented with different concentrations of PdCl<sub>2</sub> (10, 20, 30, 40 µM) for 2 hours 30 min. Cells were washed twice with phosphate buffered saline (PBS) before incubating with 10 µM **1** in PBS for 30 min at 25°C. The cells were again washed twice with PBS before imaging. Confocal imaging of MCF7 cells was achieved using NIKON AIR confocal laser scanning microscope using diode laser with excitation at 405 nm. Imaging was carried out with Plan Apo 40X objective lens.

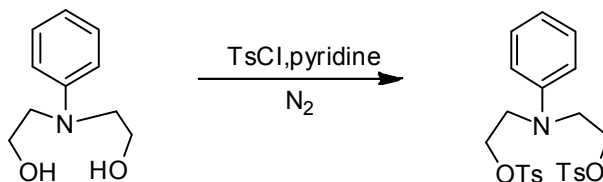
## Synthesis and characterization of compounds

### Synthesis of N,N-di( $\beta$ -hydroxyethyl) aniline.



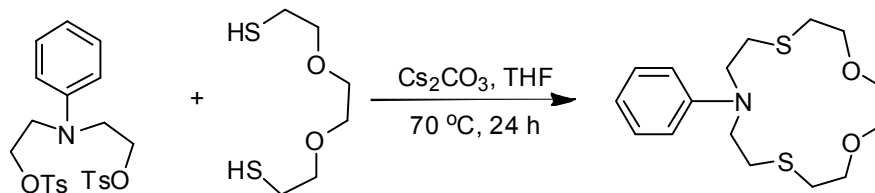
Aniline (0.10 mol, 9.31 g, 9.1 ml) was mixed with chloroethanol (0.40 mol, 26.8 ml) in 65 ml distilled water and 15.0 g  $\text{CaCO}_3$  was added to it. The resulting mixture was refluxed for 20 hours at  $100^\circ\text{C}$ , after which the reaction mixture was filtered. The filtrate was extracted with ethyl acetate after washing with brine and finally dried over anhydrous  $\text{Na}_2\text{SO}_4$ . The solvent was evaporated in vacuum to give the crude residue which was then purified by column chromatography to obtain the pure product. Yield: 86%. M.pt.  $98\text{-}103^\circ\text{C}$ .  $^1\text{H}$  NMR (300 MHz,  $\text{CDCl}_3$ , ppm)  $\delta$ : 3.55 (t,  $J = 4.8$  Hz, 4H,  $\text{CH}_2$ ), 3.79-3.82 (m, 6H,  $\text{CH}_2$ ), 6.66-6.75 (m, 3H, ArH), 7.18-7.25 (m, 2H, ArH). Anal. calcd. for  $\text{C}_{10}\text{H}_{15}\text{NO}_2$ : C, 66.30; H, 8.29; N, 7.73%. Found: C, 66.32; H, 8.34; N, 7.78%. EIMS:  $m/z$  182  $[\text{M}+1]^+$ .

### Synthesis of N,N-bis[2-(p-tolylsulphoxy)ethyl]benzenamine.



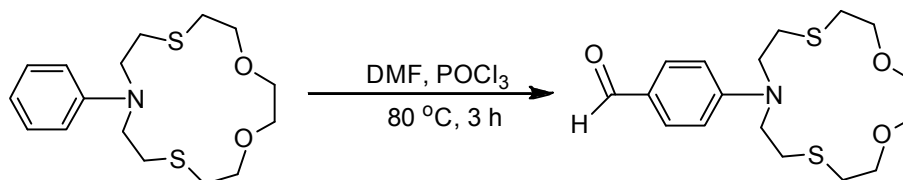
Dry compound N,N'-phenyldiethanolamine (250 mmol, 46 g) and 120 mL of anhydrous pyridine were added to a 500-mL three necked round-bottomed flask placed in an ice-salt bath, and then 96 g (500 mmol) of p-toluenesulphonyl chloride was introduced with vigorous stirring under nitrogen atmosphere. Stirring was continued for 4 h, during which the temperature was controlled to  $-5$  to  $5^\circ\text{C}$ . A yellow solid crystallized after the reaction solution was poured to 2 L of ice-water. The crystal was filtered, washed with ice-water and dried over anhydrous sodium sulfate. Recrystallization from ethanol afforded white crystalline product in 60% yield. M.pt.  $91\text{-}92^\circ\text{C}$ .  $^1\text{H}$  NMR (300 MHz,  $\text{CDCl}_3$ , ppm)  $\delta$ : 2.42 (s, 6H,  $\text{CH}_3$ ), 3.58-3.55 (t, 4H,  $\text{NCH}_2$ ), 4.12-4.09 (t, 4H,  $\text{OCH}_2$ ), 6.53-6.51 (d, 2H, ArH), 6.78-6.76 (t, 1H, ArH), 7.18-7.14 (t, 2H, ArH), 7.29-7.27 (d, 4H, ArH), 7.72-7.69 (d, 4H, ArH). Anal. calcd. For  $\text{C}_{12}\text{H}_{27}\text{O}_6\text{S}_2\text{N}$ : C, 58.89; H, 5.5; S, 13.08; N, 2.86%. Found: C, 58.59; H, 5.4; S, 13.12; N, 2.91%. EIMS  $m/z$ : 490  $[\text{M}+1]^+$ .

### Synthesis of 10-phenyl-1,4-dioxo-7,13-dithia-10-azacyclopentadecane.



Cs<sub>2</sub>CO<sub>3</sub> (1.4 g, 4.28 mmol) and 2,2'-(ethane-1,2-diylbis(oxy)) diethanethiol (1.63 mmol, 297 mg) was added to 200 ml dry THF and mixed for a one-hour. To this solution N, N-bis(2-(p-tolylsulfonyl) ethyl)-benzamine was added dropwise in 3 hours. The reaction was refluxed for 24 hours. The final compound was filtered and filtrate was concentrated in vacuum. Finally, the product was purified by silica gel chromatography (2:1 hexane/EtOAc) and eluent was removed under reduced vacuum to yield a white compound, 10-phenyl-1,4-dioxo-7,13-dithia-10-azacyclopentadecane, (400 mg, yield 75%). M.pt. 60-65°C. <sup>1</sup>H NMR (300 MHz, CDCl<sub>3</sub>, ppm) δ: 7.19 (t, *J* = 8.0 Hz, 2H, ArH), 6.62-6.57 (m, 3H, ArH), 3.72 (t, *J* = 5.2 Hz, 4H, CH<sub>2</sub>), 3.57-3.53 (m, 8H, CH<sub>2</sub>), 2.82 (t, *J* = 7.6 Hz, 4H, CH<sub>2</sub>), 2.69 (t, *J* = 5.2 Hz, 4H, CH<sub>2</sub>). Anal. calcd. For C<sub>16</sub>H<sub>25</sub>O<sub>2</sub>S<sub>2</sub>N: C,58.71; H,7.64; S,19.57; N,4.28% Found: C,58.55; H,7.44; S,19.22; N,4.91%. EIMS *m/z* 328 [M+1]<sup>+</sup>.

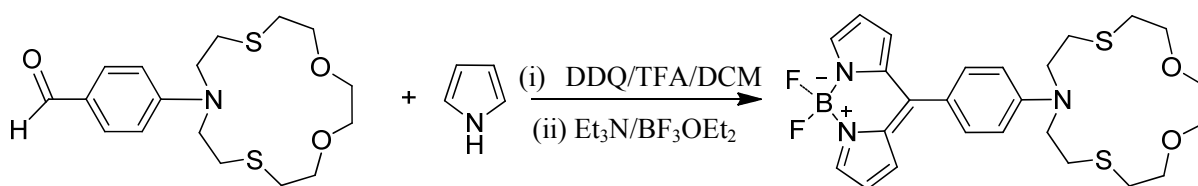
### Synthesis of 4-(1,4-dioxo-7,13-dithia-10-azacyclopentadecan-10-yl) benzaldehyde.



10 ml of dry DMF was cooled to 0 °C and POCl<sub>3</sub> (1.2mmol, 0.120 mL) was added within 5 minutes to this cooled solution. The mixture was stirred for 30 minute in ice-bath and 10-phenyl-1,4-dioxo-7,13-dithia-10-azacyclopentadecane (0.92 mmol, 300 mg) was added to it. The resulting mixture was heated for 3h at 80°C under argon. The appearance of a dark brownish color inferences the completion of the reaction which is then cooled to room temperature and-hydrolyzed by slow addition of ice-cold water followed by 5M NaOH. The product was extracted with diethyl ether. It was concentrated under vacuum and the product was purified with a column chromatography (3:1 Hexane/EtOAc) to yield the desired compound, as a yellow glass like crystals (310 mg, yield 95%). M.pt. 90-95°C. <sup>1</sup>H NMR (300 MHz, CDCl<sub>3</sub>, ppm) δ: 9.80 (s, 1H, O=C-H), 7.70 (d, *J*=8.01 Hz, 2H, ArH), 6.62 (d, *J*=8.01 Hz, 2H, ArH), 3.73

(t,  $J=5.05$  Hz, 4H, CH<sub>2</sub>), 3.60 (m, 8H, CH<sub>2</sub>), 2.84 (t,  $J=5.1$  Hz, 4H, CH<sub>2</sub>), 2.69 (t,  $J=5.04$  Hz, 4H, CH<sub>2</sub>). <sup>13</sup>C NMR (75 MHz, CDCl<sub>3</sub>)  $\delta$ : 190.9, 153.2, 134.4, 126.2, 114.2, 76.4, 70.2, 53.7, 32.2, 29.5. Anal. calcd. For C<sub>17</sub>H<sub>25</sub>O<sub>3</sub>S<sub>2</sub>N: C, 57.41; H, 7.04; S, 18.02; N, 3.94%. Found: C, 57.55; H, 7.39; S, 17.89; N, 3.91%. EIMS.  $m/z$  356 [M+1]<sup>+</sup>.

### Synthesis of Bodipy dye 1



To a solution of pyrrole (0.18 g, 1.89 mmol) and (1,4-dioxo-7,13-dithia-10-azacyclopentadecan-10-yl) benzaldehyde (0.25 mg, 0.73 mmol) in dried dichloromethane, 2 drops of CF<sub>3</sub>CO<sub>2</sub>H was added. The red solution was stirred for 3 h at room temperature under N<sub>2</sub>. After completion of the reaction (TLC), a solution of DDQ (0.47 g, 1.89 mmol) in CH<sub>2</sub>Cl<sub>2</sub> (100 mL) was added slowly through cannula addition under N<sub>2</sub>. After stirring for 30 min, Et<sub>3</sub>N (7eq) and BF<sub>3</sub>·OEt<sub>2</sub> (7eq) were subsequently added. The solution was washed with water, and the organic layer was dried over anhydrous NaSO<sub>4</sub>. Removal of the organic solvent *in vacuo* afforded a reddish solid which was purified by column chromatography on silica gel with EtOAc-hexane (2:1) as eluents to afford 0.29 g (70%) of **1**. M.pt. > 200°C. <sup>1</sup>H NMR (400 MHz, CD<sub>3</sub>CN, ppm)  $\delta$ : 7.83 (s, 2H, ArH), 7.58 (d,  $J = 9.01$  Hz, 2H, ArH), 7.12 (s, 2H, ArH), 6.83 (d,  $J = 9.01$  Hz, 2H, ArH), 6.60 (s, 2H, ArH), 3.77-3.74 (m, 8H, CH<sub>2</sub>), 3.61 (s, 4H, CH<sub>2</sub>), 2.92 (t,  $J = 7.8$  Hz, 4H, CH<sub>2</sub>), 2.74 (t,  $J = 5.1$  Hz, 4H, CH<sub>2</sub>). <sup>13</sup>C NMR (100 MHz, CDCl<sub>3</sub>, ppm)  $\delta$ : 149.7, 148.5, 141.9, 134.4, 133.5, 131, 121.9, 111.9, 111.3, 74.6, 70.8, 51.9, 31.4, 29.6. Anal. calcd. For C<sub>25</sub>H<sub>30</sub>O<sub>2</sub>S<sub>2</sub>NBF<sub>2</sub>: C, 58.02; H, 5.80; S, 12.37; N, 8.12%. Found: C, 58.06; H, 5.60; S, 12.44; N, 8.13%. EIMS.  $m/z$  518 [M+1]<sup>+</sup>.

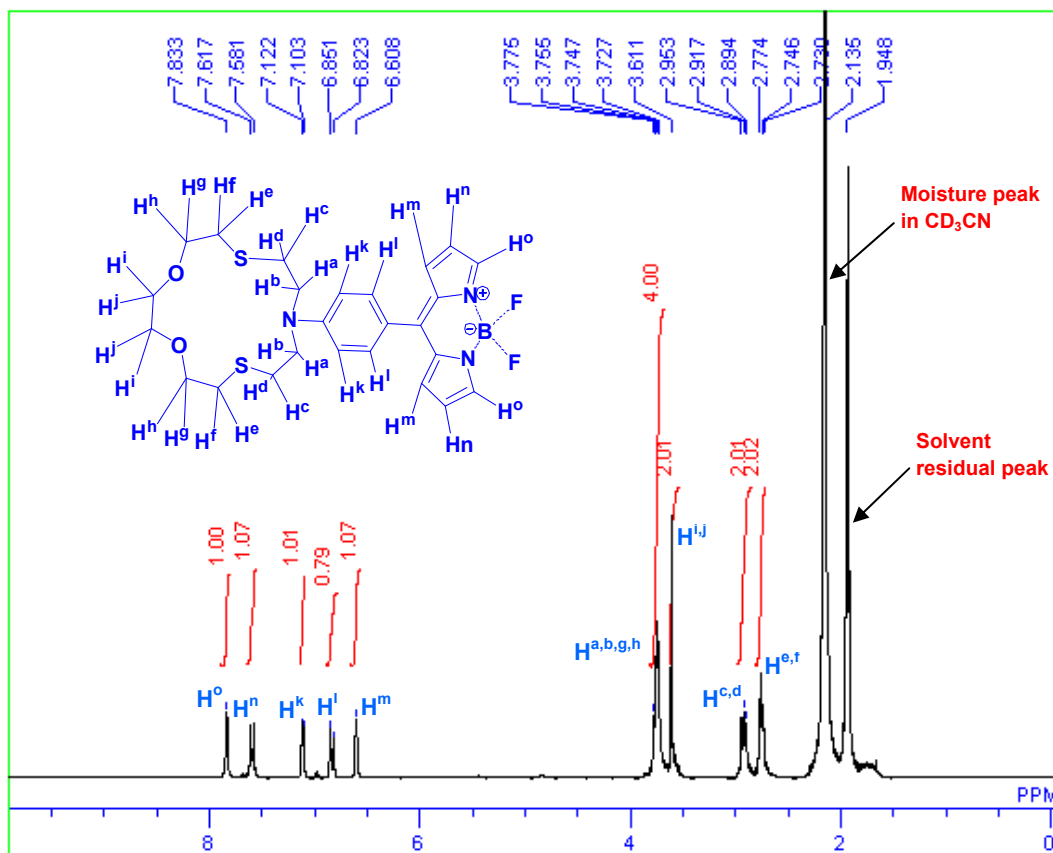


Fig. S1 <sup>1</sup>H NMR spectrum of **1** in CD<sub>3</sub>CN.

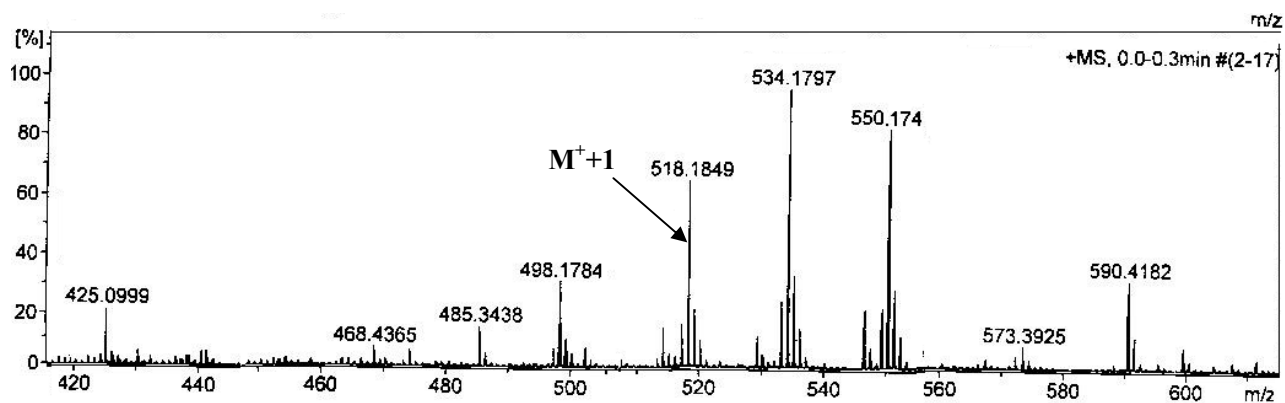


Fig. S2 Mass spectrum of **1** (solid).



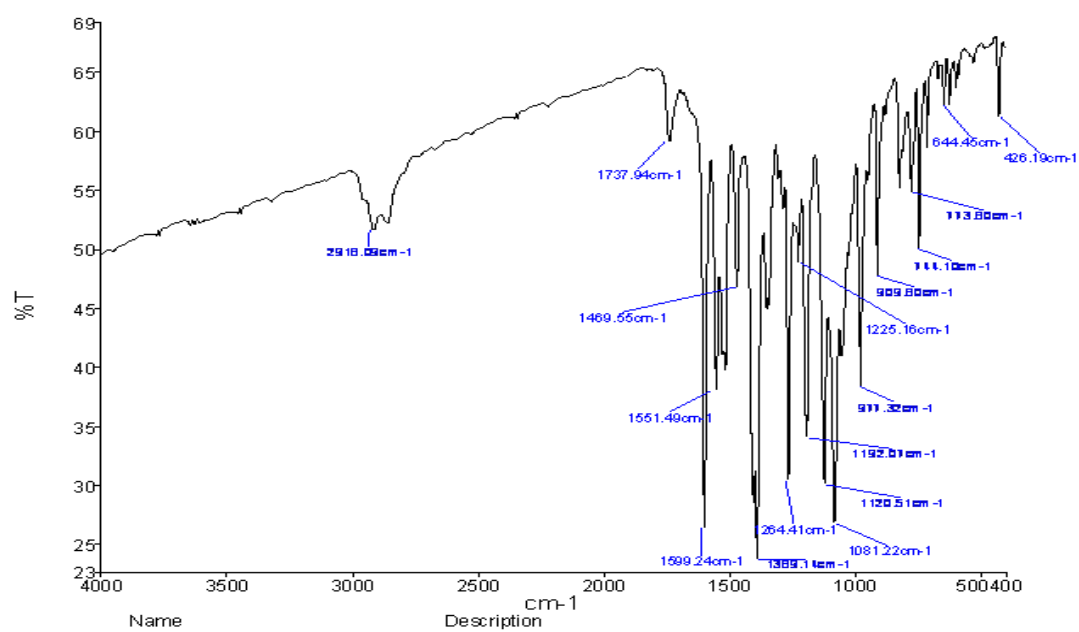


Fig. S3 IR (KBr) spectrum of 1.

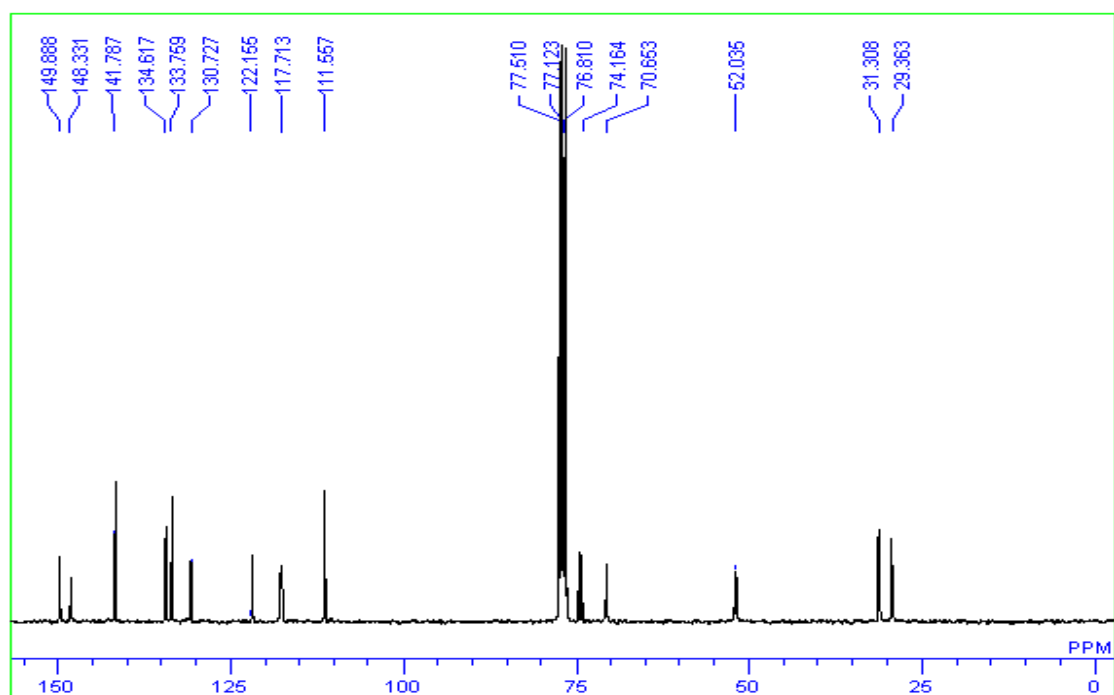
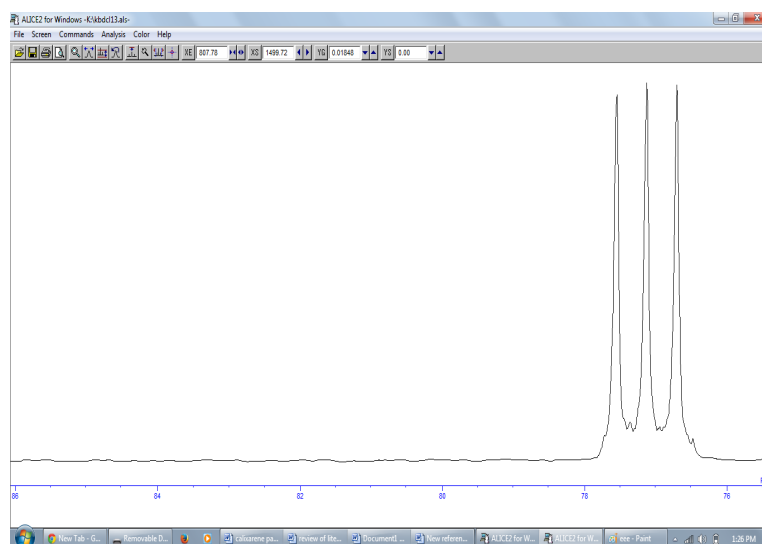
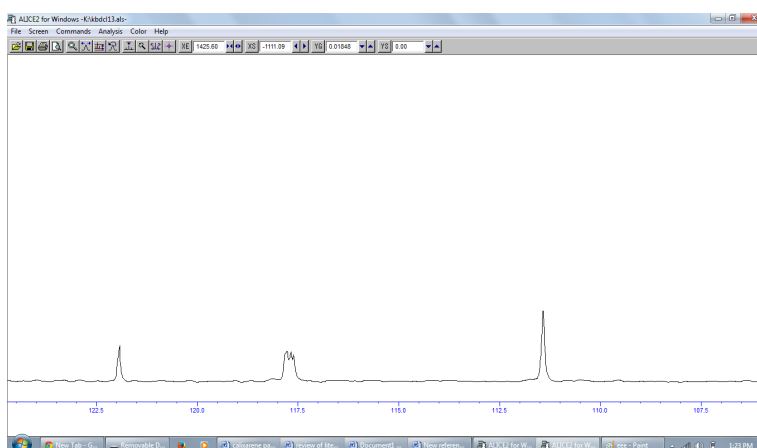
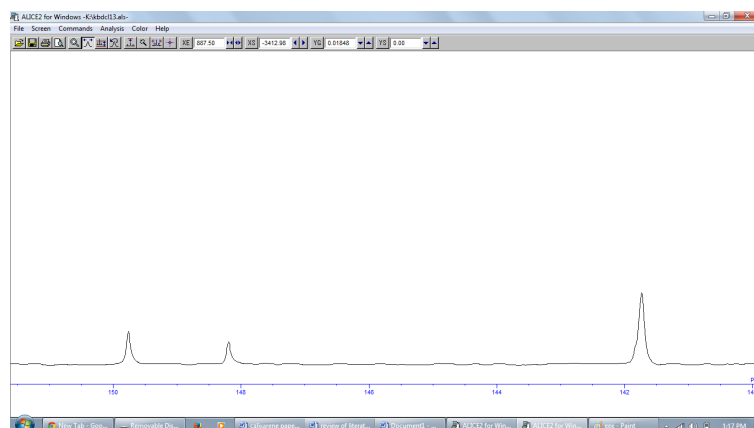
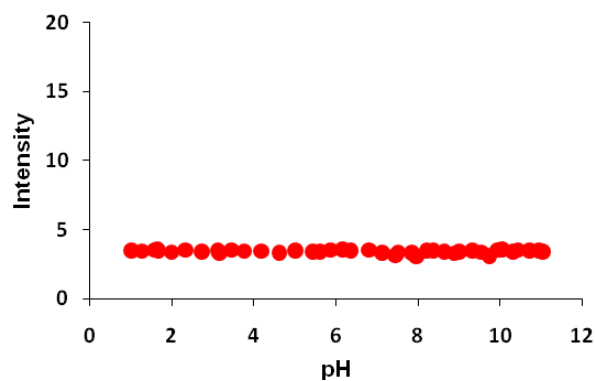


Fig. S4 <sup>13</sup>C NMR spectrum of 1 in CDCl<sub>3</sub>.



**Fig. S4a** Expanded  $^{13}\text{C}$  NMR spectrum (in part) copied from the original software (Alice).



**Fig. S5** The emission spectral pattern of **1** ( $5 \times 10^{-6}$  M, in  $\text{CH}_3\text{CN}$ ) upon pH titrations with HCl (0.01 M) and NaOH (0.01 M) in  $\text{CH}_3\text{CN}$  at 520 nm.

**Table S1.** Selected data of electronic transitions in **1** by TD-DFT calculations using B3LYP/Gen method.

$\lambda(\text{nm})$	$f^a$	Composition of bands and $\text{CI}^b$ coefficients
635	0.0003	H-6 $\rightarrow$ L, 0.45; H-5 $\rightarrow$ L, 0.80
369	0.0012	H-14 $\rightarrow$ L, 0.98
342	0.0007	H-12 $\rightarrow$ L, 0.99

<sup>a</sup> $f$ - oscillator strength, <sup>b</sup> $\text{CI}$ - configurational intergration coefficient, H - HOMO, L - LUMO

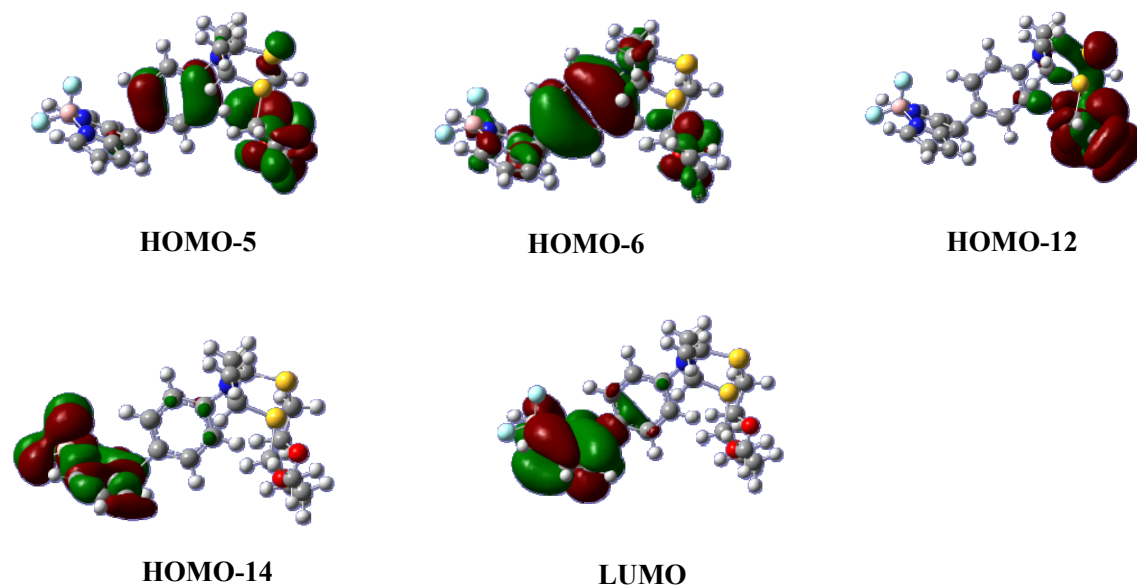
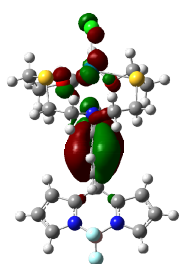


**Fig. S6** Frontier molecular orbitals of **1** contributing to UV-visible absorption bands (isovalue = 0.03).

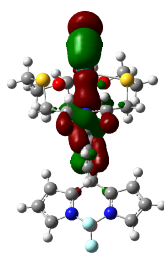
**Table S2.** Selected data of electronic transitions in  $1:\text{Pd}^{2+}$  by TD-DFT calculations using B3LYP/Gen method.

$\lambda$ (nm)	$f^a$	Composition of bands and CI <sup>b</sup> coefficients
420.74	0.0368	H-11 $\rightarrow$ L, 0.76
415.18	0.0721	H-15 $\rightarrow$ L, 0.59
391.13	0.1577	H-13 $\rightarrow$ L 0.69

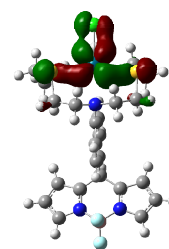
<sup>a</sup> $f$ - oscillator strength, <sup>b</sup>CI- configurational intergration coefficient, H - HOMO, L - LUMO



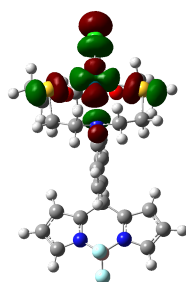
**HOMO-11**



**HOMO-13**



**HOMO-15**



**LUMO**

**Fig. S7** Frontier molecular orbitals of  $1:\text{Pd}^{2+}$  contributing to UV-visible absorption bands (isovalue = 0.03).

**Table S3:** Cartesian coordinates of **1**.

SCF Done: E(B3LYP) = -2296.5020928 a.u. after 11 cycles

Center	Atomic	Coordinates (Angstroms)		
Number	Number	X	Y	Z
1	6	0.522259	-0.231644	1.918820
2	6	-0.739541	-0.079895	1.347137
3	6	-0.835646	0.067629	-0.027431
4	6	0.309387	0.063503	-0.813128
5	6	1.563644	-0.096996	-0.245228
6	6	1.661174	-0.243942	1.135881
7	1	0.617310	-0.345984	2.984121
8	1	-1.807862	0.189854	-0.467406
9	1	0.212230	0.174840	-1.879894
10	1	2.622056	-0.373085	1.599556
11	7	-1.935065	-0.069257	2.129108
12	1	-3.047891	-1.149168	3.492842
13	1	-1.330509	1.297972	3.637904
14	6	-2.638461	-2.434173	1.826660
15	6	-2.276178	2.402109	2.080912
16	6	-2.234017	-1.323719	2.799383
17	6	-2.139182	1.129983	2.921369
18	1	-1.392641	-1.685432	3.392712
19	1	-3.045211	0.993516	3.499354
20	1	-2.612983	3.385024	2.346814
21	1	-2.285030	3.254208	2.750054
22	1	-1.421347	2.511467	1.427830

23	1	-1.928300	-2.485635	1.012480
24	16	-4.312711	-2.146417	1.172135
25	16	-3.793062	2.397334	1.069786
26	6	-4.313645	-3.160606	-0.333189
27	6	-3.256817	3.227112	-0.461119
28	1	-5.357949	-3.318713	-0.572076
29	1	-2.199842	3.050511	-0.613040
30	6	-3.626003	-2.543105	-1.541531
31	6	-4.013715	2.695413	-1.670277
32	1	-3.672520	-3.255915	-2.366710
33	1	-2.575525	-2.349821	-1.337228
34	1	-5.082274	2.665607	-1.469242
35	1	-3.857673	3.372300	-2.510933
36	8	-4.277436	-1.360882	-1.882039
37	8	-3.538727	1.423645	-1.984430
38	6	-3.783619	-0.698003	-3.002012
39	6	-4.255416	0.739081	-2.966420
40	1	-2.696159	-0.713918	-3.018332
41	1	-4.138032	-1.177482	-3.914430
42	1	-5.319971	0.758597	-2.750382
43	1	-4.097320	1.200654	-3.941552
44	6	2.816630	-0.097441	-1.131010
45	1	2.475539	-0.053702	-2.160616
46	6	3.201761	2.537897	-1.268220
47	6	5.118392	2.519893	-0.139142
48	6	4.187029	3.354816	-0.795074

49	1	2.318971	2.798275	-1.815109
50	1	6.033117	2.764590	0.357516
51	1	4.261807	4.417711	-0.894046
52	6	3.542830	-2.558550	-1.480542
53	6	4.669753	-3.319065	-1.062915
54	1	2.717170	-2.897584	-2.075293
55	6	5.458779	-2.482372	-0.338399
56	1	4.869757	-4.348280	-1.283621
57	1	6.399950	-2.661835	0.137916
58	6	3.709644	-1.304715	-0.979184
59	6	3.573652	1.173128	-0.880443
60	7	4.883297	-1.248519	-0.280077
61	7	4.701185	1.217000	-0.217740
62	5	5.434345	-0.050814	0.466904
63	9	6.777049	0.127866	0.299929
64	9	5.089745	-0.015497	1.797385
65	1	-3.414335	4.296340	-0.383308
66	1	-3.877827	-4.131482	-0.123643

**Table S4:** Cartesian coordinates of **1**:Pd<sup>2+</sup> complex.

SCF Done: E (B3LYP) = -2895.00352667 a.u. after 8 cycles

Centre Number	Atomic Number	Co-ordinates		
		X	Y	Z
1.	6	1.25068800	0.08066700	-1.80337900
2.	6	0.01461300	-0.03702200	-1.15273700
3.	6	-0.01054900	-0.16593200	0.23362800
4.	6	1.18200600	-0.18254600	0.95802000

5.	6	2.40872100	-0.06201900	0.30811000
6.	6	2.43994900	0.07181900	-1.08450900
7.	1	1.29591900	0.17319100	-2.87018100
8.	1	-0.94351800	-0.26804900	0.74519600
9.	1	1.13517800	-0.29465600	2.02503700
10.	1	3.36809500	0.16191300	-1.61701300
11.	7	-1.22990400	-0.06223400	-1.89823100
12.	1	-2.31447000	0.97822600	-3.34875300
13.	1	-0.61693800	-1.42254800	-3.42183600
14.	6	-1.59062100	2.44119500	-1.94537300
15.	6	-1.38625900	-2.60002200	-1.81465000
16.	6	-1.42972200	1.14457500	-2.75099000
17.	6	-1.40135000	-1.32824500	-2.67135100
18.	6	-0.60144300	1.26972800	-3.44466100
19.	1	-2.34239300	-1.26107900	-3.19796000
20.	1	-1.43696600	3.29036600	-2.59283600
21.	1	-1.37374300	-3.45725800	-2.46948800
22.	1	-0.51407700	-2.64304200	-1.18151100
23.	1	-0.87819200	2.48696400	-1.13783400
24.	S	-3.33123200	2.54551200	-1.25974400
25.	16	-2.91830900	-2.74329200	-0.73945200
26.	6	-3.20779600	3.49277600	0.35036200
27.	6	-2.27443000	-3.29378600	0.94557900
28.	1	-4.21846400	3.44239200	0.72438200
29.	1	-1.20612000	-3.14291400	0.96911100
30.	6	-2.23659400	2.95297000	1.39512600



31.	6	-2.93699100	-2.53476300	2.08846100
32.	1	-2.38253900	3.52800100	2.30555400
33.	1	-1.20410400	3.08346400	1.08534400
34.	1	-3.99714800	-2.40863900	1.91389500
35.	1	-2.79906700	-3.09624900	3.00797300
36.	8	-2.48758300	1.56700500	1.63435900
37.	8	-2.30803400	-1.24651700	2.22986100
38.	6	-2.34978700	1.05234900	2.96860200
39.	6	-3.02696800	-0.29949700	3.05072100
40.	1	-1.29716800	0.97485200	3.22792700
41.	1	-2.83226200	1.72398500	3.67195500
42.	1	-4.04560900	-0.22054600	2.70272600
43.	1	-3.01407300	-0.63996600	4.08265600
44.	6	3.71627600	-0.08979200	1.12347800
45.	1	3.44738500	-0.18550600	2.16818300
46.	6	4.29631800	-2.69505600	1.03924100
47.	6	6.22692700	-2.46381500	-0.10363900
48.	6	5.34348800	-3.40343900	0.50266700
49.	1	3.44494100	-3.06545600	1.56501500
50.	1	7.14980900	-2.61611500	-0.61611800
51.	1	5.49060700	-4.45869900	0.52557900
52.	6	4.14716400	2.52149800	1.47890500
53.	6	5.15075200	3.36734200	1.07480900
54.	1	3.27845000	2.74998900	2.05465000
55.	6	6.08327900	2.59360800	0.32445700
56.	1	5.23876000	4.41031600	1.27527600

57.	1	6.99426600	2.88102400	-0.14992800
58.	6	4.48433200	1.19222800	0.96017000
59.	6	4.55568100	-1.28088900	0.75199500
60.	7	5.63069100	1.27897600	0.28344700
61.	7	5.70127000	-1.18821600	0.07465800
62.	5	6.30897100	0.12078100	-0.49901300
63.	9	7.68726100	0.14319100	-0.29184300
64.	9	5.97703000	0.22745900	-1.86101600
65.	1	-2.48887400	-4.34774800	1.02479100
66.	1	-2.96760200	4.52016000	0.11893000
67.	46	-3.53486800	-0.09260700	-0.52377000
68.	17	-5.78469100	-0.25119300	0.66507000

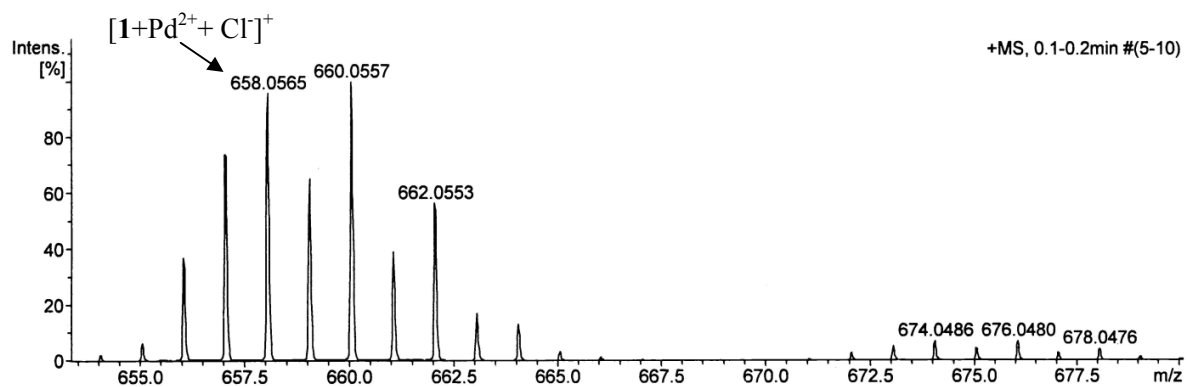


**Fig. S8** Mass spectrum of  $1: Pd^{2+}$  complex.

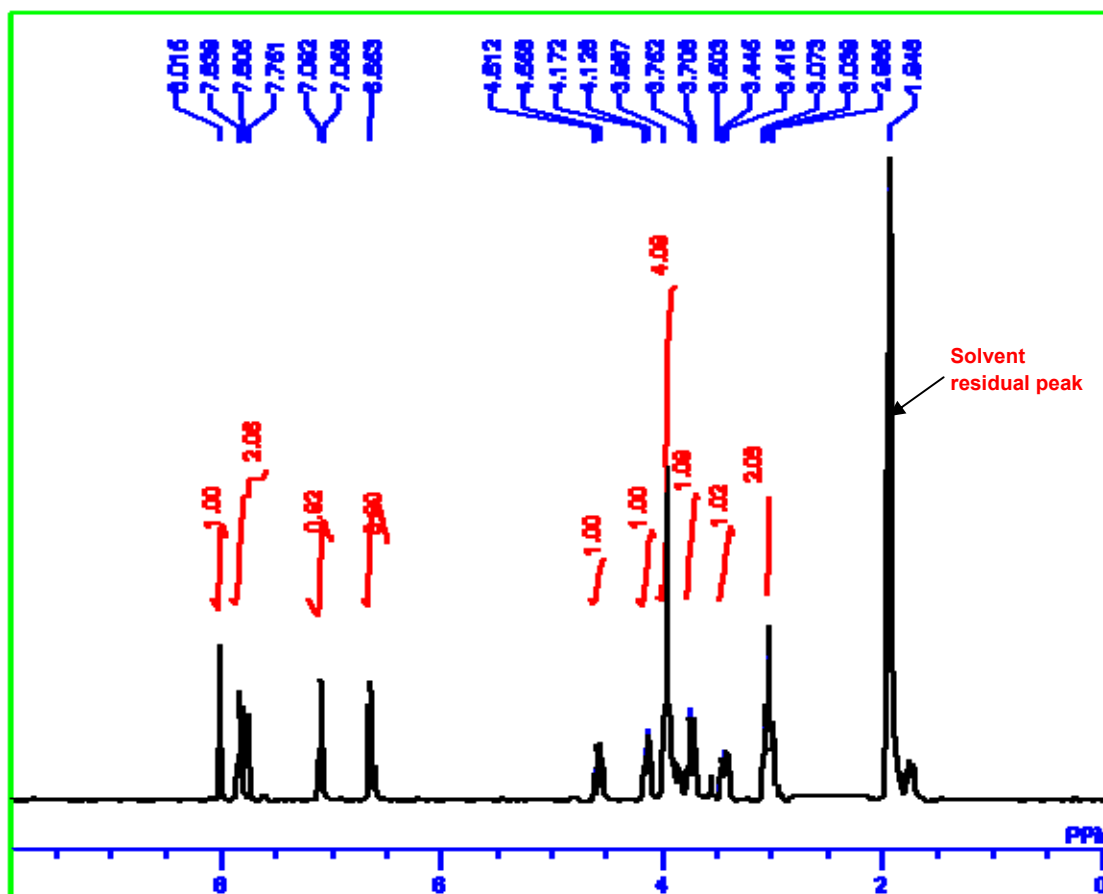
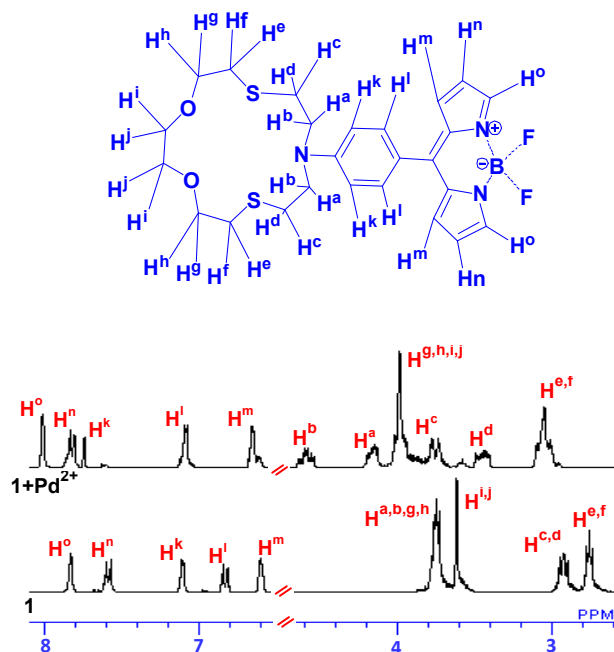


Fig. S9  $^1\text{H}$  NMR of  $1:\text{Pd}^{2+}$  complex (**1** in  $\text{CD}_3\text{CN}$  and  $\text{Pd}^{2+}$  as  $\text{PdCl}_2$  in  $d_6$ -DMSO).

Table S5. Changes in the  $^1\text{H}$  NMR spectrum of **1** (in  $\text{CD}_3\text{CN}$ ) upon addition of  $\text{Pd}^{2+}$  (in  $d_6$ -DMSO), immediately after the addition. Full spectra in (Fig. S1 and S10).

	<b>1</b>	<b>1</b> : $\text{Pd}^{2+}$
$\text{H}^a$	3.75	4.31
$\text{H}^b$		4.58
$\text{H}^c$	2.92	3.75
$\text{H}^d$		3.49
$\text{H}^e$	2.75	3.03
$\text{H}^f$		
$\text{H}^g$	3.75	3.98
$\text{H}^h$		
$\text{H}^i$	3.60	3.98
$\text{H}^j$		
$\text{H}^k$	7.12	7.80
$\text{H}^l$	6.83	7.08
$\text{H}^m$	6.60	6.65
$\text{H}^n$	7.58	7.83
$\text{H}^o$	7.83	8.01



**Table. S6** Representative detection limits for Pd<sup>2+</sup> reported by various research groups

S. No.	Detection Limit	Mode of Action	Reference
1	0.11 ppm	Ligation	4
2	0.4 ppb	chemodosimeter	5
3	0.16 ppb	ligation	6
4	0.55 ppb	chemodosimeter	7
5	4.28 ppb	chemodosimeter	8
6	0.11 ppm	ligation (aggregation)	9
7	29.96 ppb	ligation	10
8	9.30 ppb	chemodosimeter	11
9	0.10 ppm	chemodosimeter	12
10	7.49 ppb	chemodosimeter	13
11	0.65 ppb	chemodosimeter	14
12	0.58 ppm	chemodosimeter	15
13	19.7 ppb	chemodosimeter	16
14	0.42 ppm	chemodosimeter	17

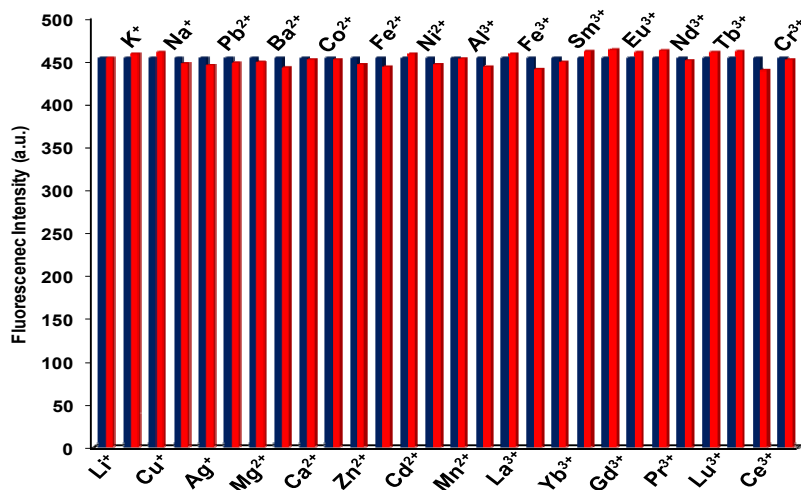


**Fig. S10** Changes in the emission properties of **1** ( $5 \times 10^{-6}$  M, in CH<sub>3</sub>CN at 520 nm) upon addition of Pd<sup>2+</sup> ( $2.28 \times 10^{-5}$  M, H<sub>2</sub>O:DMSO, 9:1 v/v) in the presence of other cations ( $2.28 \times 10^{-5}$  M in water), in CH<sub>3</sub>CN.

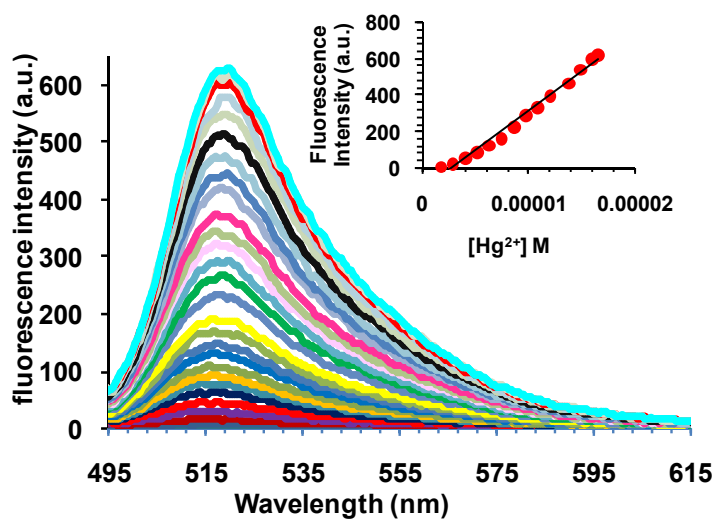


**Fig. S11** Changes in the emission spectrum of **1** ( $5 \times 10^{-6}$  M, in CH<sub>3</sub>CN) upon addition of different concentrations of Hg<sup>2+</sup> ( $2.87 \times 10^{-7}$  M -  $1.14 \times 10^{-5}$  M in water) in CH<sub>3</sub>CN.

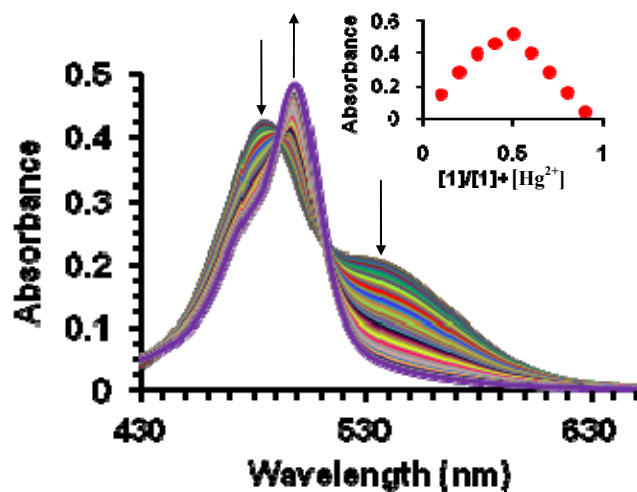


**Fig. S12** Changes in the absorption spectrum of **1** ( $1 \times 10^{-5}$  M, in CH<sub>3</sub>CN) upon addition of different concentrations of Hg<sup>2+</sup> ( $2.85 \times 10^{-7}$  -  $2.28 \times 10^{-5}$  M in water), in CH<sub>3</sub>CN.

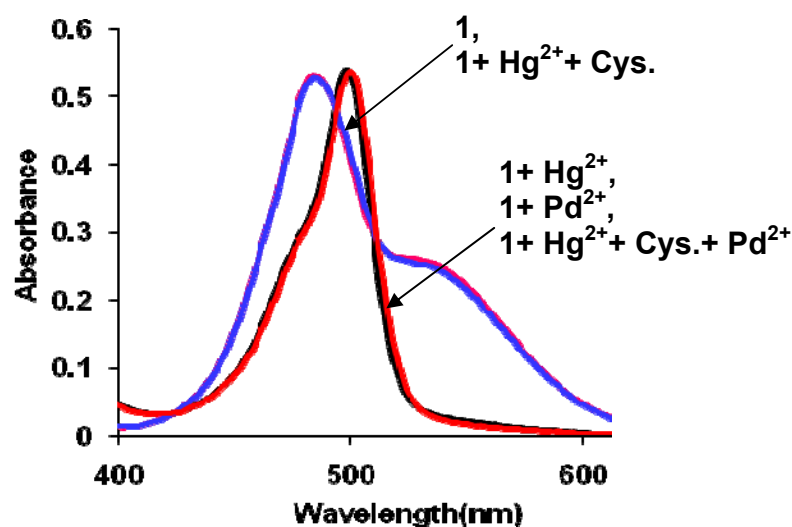
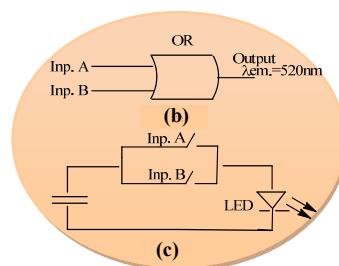


**Fig. S13** Changes in the absorption spectra of **1**, upon sequential addition of  $\text{Hg}^{2+}$  ( $2.28 \times 10^{-5}$  M in water), cysteine ( $5.1 \times 10^{-6}$  M in water) and  $\text{Pd}^{2+}$  ( $1.54 \times 10^{-5}$  M,  $\text{H}_2\text{O}:\text{DMSO}$ , 9:1 v/v) into solution of **1** ( $1 \times 10^{-5}$  M in  $\text{CH}_3\text{CN}$ ) in  $\text{CH}_3\text{CN}$ .

Additionally, the behaviour of **1** in the presence of  $\text{Pd}^{2+}$  and  $\text{Hg}^{2+}$  was also implemented to generate a fundamental OR logic gate for which the corresponding *truth table*, symbol and the electric circuit are shown in figure below. The electric circuit for OR gate has switches in parallel connected to load LED and source battery. When both the switches are open, current does not flow to LED, but when any system is closed, the current flows. The generation of fundamental gates is important to achieve the progress in the development of complicated circuits.

Inp. A ( $\text{Pd}^{2+}$ )	Inp. B ( $\text{Hg}^{2+}$ )	Output $\lambda_{\text{em.}}$ 520 nm
0	0	0
1	0	1
0	1	1
1	1	1

(a)



(c)

**Fig. S14 (a)** *Truth table*, **(b)** symbol and **(c)** electric circuit for OR logic gate. An active output i.e. 1 is obtained when any of the inputs is active i.e. 1.

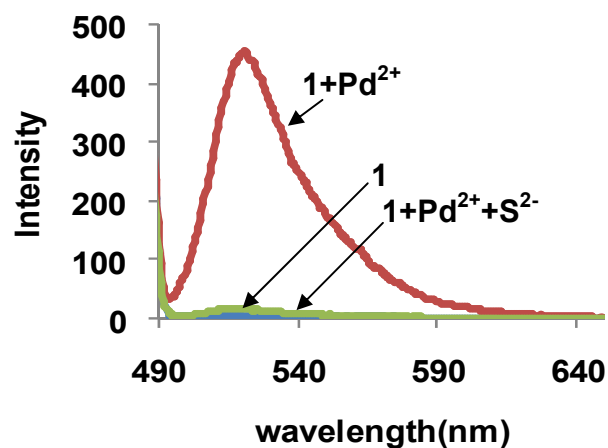


**Fig. S15** Changes in the emission spectrum of **1** ( $5 \times 10^{-6}$  M in CH<sub>3</sub>CN), **1** in the presence of Pd<sup>2+</sup> ( $2.28 \times 10^{-5}$  M, in DMSO:H<sub>2</sub>O, 9:1 v/v) and upon addition of S<sup>2-</sup> ( $5.71 \times 10^{-6}$  M, in water) in the later, in CH<sub>3</sub>CN.

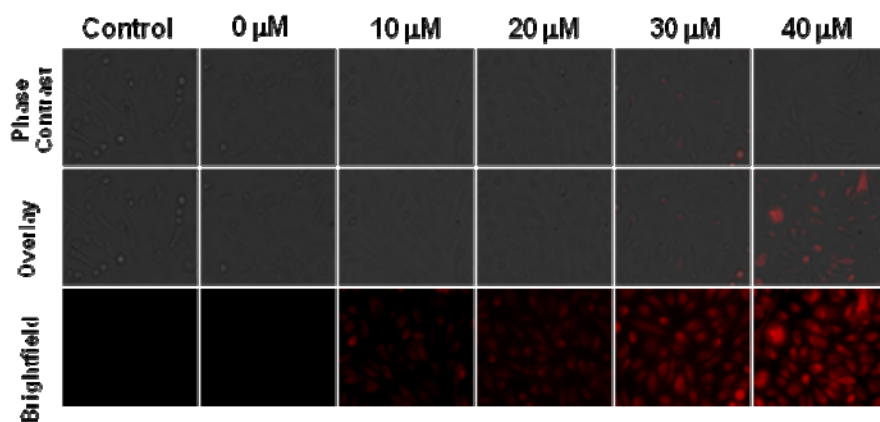


**Fig. S16** Confocal images of MCF-7 cells, supplemented with various concentration of Pd<sup>2+</sup> (10 μM, 20 μM, 30 μM and 40 μM) and **1** ( $1 \times 10^{-5}$  M).

## References:

1. J. V. Morris, M. A. Mahaney, J. R. Huber, *J. Phys. Chem. B.*, 1976, **80**, 969.
2. Gaussian 09, Revision B.01, M. J. Frisch, G. W. Trucks, H. B. Schlegel, G. E. Scuseria, M. A. Robb, J. R. Cheeseman, G. Scalmani, V. Barone, B. Mennucci, G. A. Petersson, H. Nakatsuji, M. Caricato, X. Li, H. P. Hratchian, A. F. Izmaylov, J. Bloino, G. Zheng, J. L. Sonnenberg, M. Hada, M. Ehara, K. Toyota, R. Fukuda, J. Hasegawa, M. Ishida, T. Nakajima, Y. Honda, O. Kitao, H. Nakai, T. Vreven, J. A. Montgomery, Jr., J. E. Peralta, F. Ogliaro, M. Bearpark, J. J. Heyd, E. Brothers, K. N. Kudin, V. N. Staroverov, T. Keith, R. Kobayashi, J. Normand, K. Raghavachari, A. Rendell, J. C. Burant, S. S. Iyengar, J. Tomasi, M. Cossi, N. Rega, J. M. Millam, M. Klene, J. E. Knox, J. B. Cross, V. Bakken, C. Adamo, J. Jaramillo, R. Gomperts, R. E. Stratmann, O. Yazyev, A. J. Austin, R. Cammi, C. Pomelli, J. W. Ochterski, R. L. Martin, K. Morokuma, V. G. Zakrzewski, G. A. Voth, P. Salvador, J. J. Dannenberg, S. Dapprich, A. D. Daniels, O. Farkas, J. B. Foresman, J. V. Ortiz, J. Cioslowski, and D. J. Fox, Gaussian, Inc., Wallingford CT, **2010**. (complete ref. 16).
3. L. J. Bartolotti and K. Fluchick, In *Reviews in Computational Chemistry*, K. B. Lipkowitz, B. D. Boyd, Eds, VCH, New York, 1996, Vol. 7, pp. 187.
4. J. Panchompoo, L. Aldous, M. Baker, M. I. Wallace, R. G. Compton, *Analyst*, 2012, **137**, 2054-2062.
5. J. Wang, F. Song, J. Wang, X. Peng, *Analyst*, 2013, **138**, 3667-3672.
6. S. Cai, Y. Lu, S. He, F. Wei, L. Zhaoab, X. Zeng, *Chem. Commun.*, 2013, **49**, 822-824.
7. L. Cui, W. Zhua, Y. Xua, X. Qiana, *Anal. Chim. Acta*, 2013, **786**, 139-145.
8. M. Kumar, N. Kumar, V. Bhalla, *RSC Adv.*, 2013, **3**, 1097-1102.
9. B. Liu, Y. Bao, H. Wang, F. Du, J. Tian, Q. Li, T. Wang, R. Bai, *J. Mater. Chem.*, 2012, **22**, 3555-3561.
10. Y. Zhou, J. Zhang, H. Zhou, Q. Zhang, T. Ma, J. Niu, *Sens. Actuators B*, 2012, **171-172**, 508-514.
11. B. Liu, H. Wang, T. Wang, Y. Bao, F. Du, J. Tian, Q. Li, R. Bai, *Chem. Commun.*, 2012, **48**, 2867-2869.
12. W. Chen, B. D. Wright, Y. Pang, *Chem. Commun.*, 2012, **48**, 3824-3826.



13. B. Zhu, C. Gao, Y. Zhao, C. Liu, Y. Li, Q. Wei, Z. Ma, B. Du, X. Zhang, *Chem. Commun.*, 2011, **47**, 8656-8658.
14. J. Jiang, H. Jiang, W. Liu, X. Tang, X. Zhou, W. Liu, R. Liu, *Org. Lett.*, 2011, **13**, 4922-4925.
15. S. Y. Yu, H. W. Rhee, J. I. Hong, *Tet. Lett.*, 2011, **52**, 1512-1514.
16. M. Santra, S. K. Ko, I. Shin, K. H. Ahn, *Chem. Commun.*, 2010, **46**, 3964-3966.
17. A. L. Garner, K. Koide, *J. Am. Chem. Soc.*, 2008, **130**, 16472-16473.